GEOPHYSICAL RESEARCH LETTERS, VOL. 33, L14303, doi:10.1029/2006GL026249, 2006



# Explosion energy of the 2004 eruption of the Asama Volcano, central Japan, inferred from ionospheric disturbances

Kosuke Heki[1]

Received 8 March 2006; revised 26 May 2006; accepted 7 June 2006; published 19 July 2006.

[1] The Japanese dense array of Global Positioning System recorded ionospheric disturbances as changes in Total Electron Content ~12 minutes after the September 1 2004 eruption of the Asama Volcano, Central Japan. The disturbance had a period of one and a quarter minutes and propagated as fast as ~1.1 km/s, suggesting its origin as the acoustic wave generated by the explosion. By comparing the disturbance amplitudes with those by a surface mine blast with a known energy, the overall Asama explosion energy is inferred to be about $2 \times 10^{14}$ J. **Citation:** Heki, K. (2006), Explosion energy of the 2004 eruption of the Asama Volcano, central Japan, inferred from ionospheric disturbances, *Geophys. Res. Lett.*, *33*, L14303, doi:10.1029/2006GL026249.

## 1. Introduction

[2] Ionospheric Total Electron Content (TEC) can be easily measured as the phase differences of the L band carrier waves in two frequencies from Global Positioning System (GPS) satellites. Ionospheric disturbances measured as TEC variations have been contributing to studies of solar-terrestrial physics, for example, Traveling Ionospheric Disturbances (TID) [e.g., *Tsugawa et al.*, 2004], TEC disturbances by solar eclipse [*Afraimovich et al.*, 2002] and by solar flares [*Zhang and Xiao*, 2005].

[3] *Calais and Minster* [1995] paved the way to use GPS-TEC as a sensor to study the solid earth. Targets of such studies over the last decade include the disturbances associated with atmospheric acoustic waves excited by coseismic crustal uplifts [*Heki and Ping*, 2005] and passage of Rayleigh surface waves [*Ducic et al.*, 2003], and atmospheric internal gravity waves excited by tsunamis [*Artru et al.*, 2005]. Here I present a new application of GPS-TEC, that is, estimation of the explosion energy of a volcanic eruption. This new technique would complement past methods based on observations of mass deficits, near-field measurements of airwaves, etc, and may contribute to mitigate volcanic hazards.

## 2. Data Analysis

[4] The Asama Volcano, Central Japan (Figure 1), started eruptive activity at 11:02 UT on September 1, 2004, with a vulcanian explosion associated with strong airwaves [*Nakada et al.*, 2005]. The Japanese dense GPS array GEONET (GPS Earth Observation Network), composed of ~1000 continuous GPS tracking stations, record L1 (~1.5 GHz) and L2 (~1.2 GHz) carrier phases every 30 seconds. Ionospheric delays are frequency dependent, and phase differences between the two carriers convey information on the TEC values along the line-of-sight and their changes in space and time. To detect TEC changes caused by the eruption, the lines need to penetrate the ionosphere (maximum electron density as high as ~300 km) near the volcano. This condition was met at the time of eruption by observing the satellite 15 from GPS stations in the Kansai District.

[5] Figure 1 shows five sets of TEC time series, composed of five GPS points penetrating ionosphere within 200 km in horizontal distances from the volcano in different azimuths. Clear N-shaped disturbance signals are seen 11–13 minutes after the eruption in the south- and southwestward azimuths. Faint signals are recognized in the western ionosphere, but no disturbance signals can be seen toward the northeast and east. Such asymmetry partly comes from the directivity caused by the geomagnetism [*Heki and Ping*, 2005], and partly from difference in the angle between the line-of-sight and the wavefront. These are the first detection of the ionospheric disturbances with GPS, although Doppler sounding technique has detected disturbances of volcanic origin, for example, the 1980 explosion of Mount St. Helens [*Roberts et al.*, 1982] and the 1991 Pinatubo eruption [*Igarashi et al.*, 1994].

[6] First, I try to adjust a simple function

$$f(t) = -at \exp\left(\frac{-t^2}{2\sigma^2}\right), \quad (1)$$

made of a set of positive and negative pulses, to the observed disturbances (Figure 2). The function has maximum and minimum at $t = -\sigma$ and $t = \sigma$, respectively. The two parameters $a$ and $\sigma$, representing the amplitude and period respectively, were tuned to minimize the root-mean-squares (rms) of differences between the synthesized and the observed disturbances. The values $a = 0.0070$ and $\sigma = 19$ resulted in good fits to the majority of time series, which correspond to ~0.16 TECU (1TECU = $10^{16}$ electrons/m$^2$) as the peak-to-peak amplitude (i.e., $f(-\sigma) - f(\sigma)$), and 76 seconds (about 1 and 1/4 minutes) as the approximate period (i.e., $4 \times \sigma$), respectively (Figure 2, bottom center). Disturbance arrival times were determined for individual time series by moving the source function with a time step of 2.5 seconds and finding the time lags that minimize the rms of the differences.

[7] To infer the apparent velocity of the propagating disturbances, I plot the arrival times as a function of distances (measured along the Earth's surface between the volcano and the ground projection of the ionosphere penetration point) from the volcano (Figure 2, bottom left/

[1]Department of Natural History Science, Hokkaido University, Sapporo, Japan.


0094-8276/06/2006GL026249$05.00

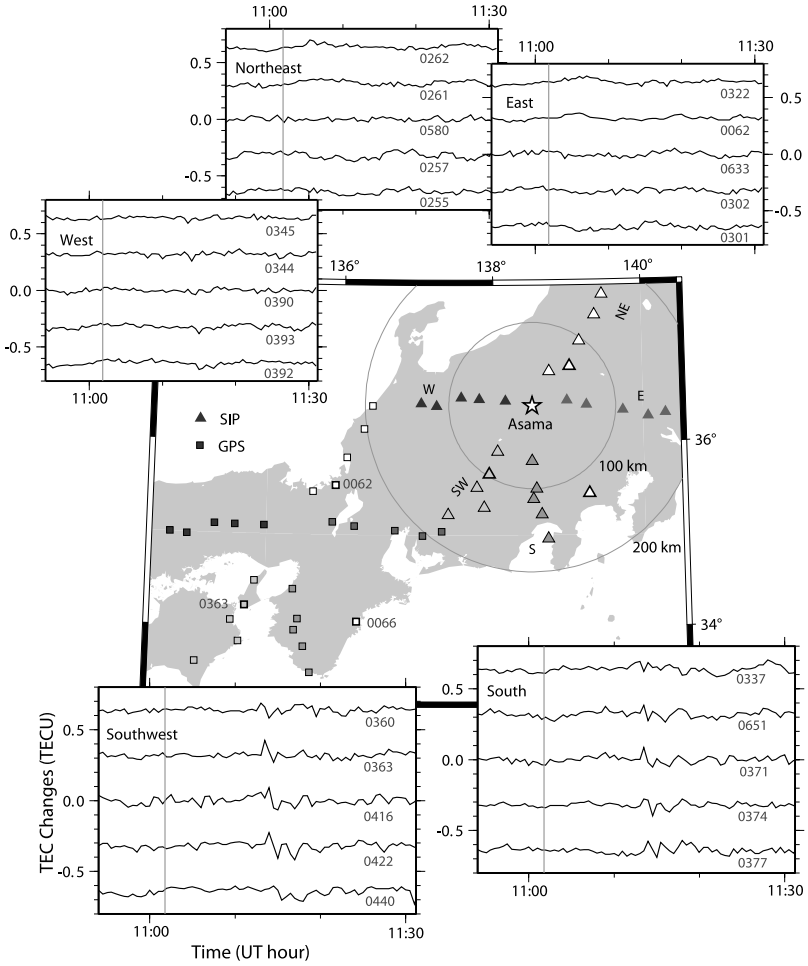


**Figure 1.** Time series of TEC (Sat. 15) for GPS stations (squares) with the ground projections of the ionosphere (height is assumed to be 300 km) piercing points (triangles) in different azimuths from the volcano (open star). There are clear disturbances in southern and southwestern stations about 10 minutes after the eruption (11:02, vertical gray lines). They are less conspicuous in the western stations and absent in northeastern and eastern stations. Numbers in the time series are the station IDs in four digits. TEC time series closer to the volcano are displayed in upper positions. Time series of the three GPS stations shown by squares with bold frames (0062, 0066, and 0363) are compared with synthesized ones in Figure 3.

right). The apparent velocities were 1.08 ± 0.05 and 1.12 ± 0.10 km/sec, similar to the sound velocity at the ionospheric height [*Fitzgerald*, 1997; *Calais et al.*, 1998]. The onset of the propagation lags behind the explosion by ∼10 minutes, which corresponds to the time required for the sound wave to travel upward from ground to ionosphere. The atmospheric sound wave would have been excited by the explosion, propagated upward reaching ionosphere, and have disturbed electron density distribution there.

[8] The period of the present case is within the window of the atmospheric filter [*Georges*, 1968]. It is interesting to note that it is significantly shorter than the typical period of coseismic ionospheric disturbances ∼4.5 minutes, one of the resonance periods between the atmosphere and the ground [*Tahira*, 1995]. To identify the physical processes governing the period is an interesting future issue.

## 3. Explosion Energy

[9] In the present study, ionospheric disturbances caused by the Asama eruption in the southern ionosphere, was 0.16 TECU in peak-to-peak amplitude. *Calais et al.* [1998], using GPS, observed ionospheric disturbances of 0.03 TECU (also in the southern azimuth) after a 1.5 Kt (ANFO explosives, similar in power to trinitrotoluene, TNT) surface mine blast at a coal mine in Wyoming, USA. By comparing these two cases, we could roughly infer the energy of the Asama explosion.

[10] At first, the differences in conditions of the two cases need to be clarified. One of the important factors is the background TEC when the explosions occurred; the wave energy would depend on TEC changes relative to the background values. Daily vertical TEC change curves obtained by analyzing GEONET data are available on line by Akinori Saito, Kyoto University, at www-step.kugi.kyoto-u.ac.jp/∼saitoua/GPS_TEC. The background TEC was ∼10 TECU for the Asama case. That for the US mine blast case is not directly available, but would be similar to the TEC of a point in Japan on the same day, at the same solar time, and latitude. It was ∼20 TECU, about twice as large as the Asama case.

[11] Another important factor is the incidence angle of the line-of-sight vector into the acoustic wavefront. In Figure 3, I show three examples, observing the northeastern (0062), southeastern (0066), and southwestern (0363) ion-

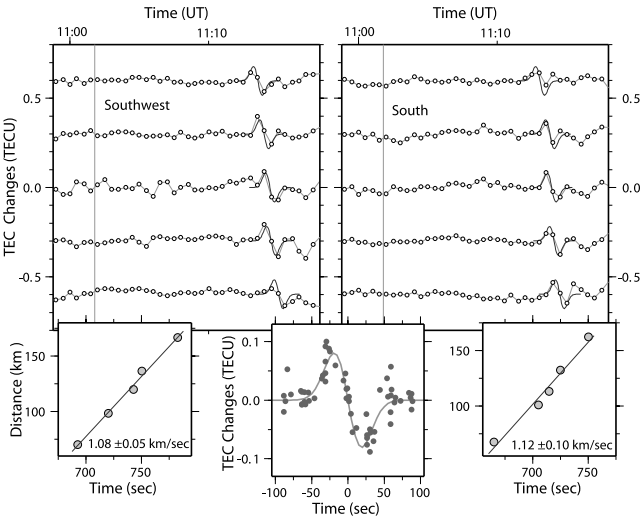


**Figure 2.** Arrival times of the disturbances are determined by searching for the time lag giving minimal differences between the source function (dark gray curves, see equation 1 of the text) and the observed TEC (open circles with the sampling interval of 30 seconds), for GPS points observing the (top left) southwestern and (top right) southern skies (Figure 1). (bottom left and right) Linear regressions are performed for the estimated arrival times, and the apparent velocities of the disturbance propagation of ∼1.1 km/s were estimated. (bottom center) Observed TEC values from the ten time series are compared with the source function after adjusting the time lags.

osphere (locations of the GPS receivers and sub-ionospheric points given in Figure 1). The upper panel shows the geometry of the wavefront and the line-of-sight. The amplitudes of the TEC disturbances are the largest for 0363, and the smallest for 0062. This difference comes from the incidence angle; that is, a shallower angle causes a larger signal, because the positive and negative parts cancel less each other. Similar calculations for the US mine blast case resulted in fairly deep incidence angles (consistent with Figure 7b of *Calais et al.* [1998]). Numerical calculation showed that the TEC signal generated by the same source function was ∼1/2 of our case of 0066.

[12] The geomagnetic inclination is deeper in the mine blast case than the Asama case by ∼20 degrees. However, difference in the directivities between the two cases, inferred from the same calculation that *Heki and Ping* [2005] performed to draw their Figure 6b, was not serious. After all, the two factors, the background TEC (twice as large), and the incidence angle (one half), influence the amplitude oppositely and would largely cancel each other. The apparent difference in the observed disturbance amplitudes hence mainly reflects the energy difference. Since wave energy scales with the square of the amplitude, the total explosion energy of the Asama eruption would be $\sim 4 \times 10^4$ t TNT, or $2 \times 10^{14}$ Joule. This is ∼1/2 of the energy reported for the 1938 eruption [*Minakami*, 1942].

## 4. Discussion

[13] Apart from the empirical approach described in the previous section, *Johnson* [2003] estimated the air wave energy of a volcanic eruption $E_{\mathrm{acoustic}}$ with a purely physical approach, that is,

$$E_{acoustic} = \frac{2\pi r^2}{\rho_{atmos} c_{atmos}} \int \Delta P(t)^2 dt \qquad (2)$$

where $\rho_{\mathrm{atmos}}$ and $c_{\mathrm{atmos}}$ are the density and the sound velocity, respectively, $r$ is the distance from the volcano, and $\Delta P$ is the pressure perturbation. Here I assume that the observed ionospheric disturbance is a part of the spherical wave propagated from the volcano. Assuming 300 km (F layer height) for $r$, $5 \times 10^{-11}$ kg/m$^3$ for $\rho_{\mathrm{atmos}}$, 1.1 km/sec for $c_{\mathrm{atmos}}$, we obtain $1.2 \times 10^7$ Joule for $E_{\mathrm{acoustic}}$. There the pressure perturbation $\Delta P$ is calculated as the product of the ambient pressure $P$ at 300 km height, and the TEC perturbation relative to the background (i.e., $\Delta P = P \times \Delta\mathrm{TEC}/\mathrm{TEC}$). This energy value is only a small portion of

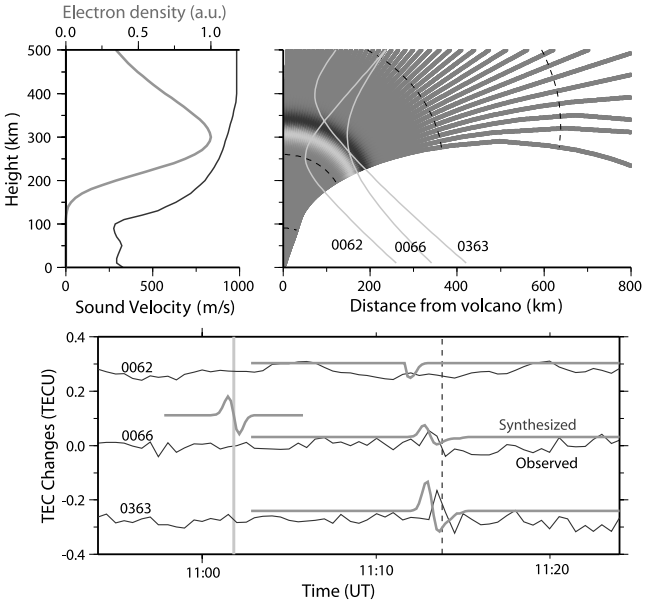


**Figure 3.** (top left) Relative electron density (light gray) and velocity of acoustic wave (dark gray) are plotted as functions of height [*Calais et al.*, 1998]. (top right) Ray tracing of acoustic waves for zenith angles 0–20 degrees is done assuming this velocity profile. Equal-time contours are shown for 5, 10, 15, and 20 minutes after the eruption with broken curves. Gray scales shown along the ray paths indicate the position of the source function at 11.23 minutes after the eruption (∼11:14 UT, broken line in the bottom panel). Gray curves are the line-of-sights connecting the satellites 15 and three GPS stations 0062, 0066, and 0363 (their positions shown in Figure 1). They are straight in 3-dimensional space, but have apparent curvatures here because we took the distance from Asama as the horizontal axis. The observed (dark gray, residuals of the polynomial fit) and synthesized (light gray, based on the ray tracing) TEC time series of the three points for satellites 15 are given in the bottom panel. The observed arrival times, waveforms, and relative amplitudes are consistent with the synthesized curves for 0066 and 0363. Absence of signals in 0062 would be due to the directivity of ionospheric disturbances [*Heki and Ping*, 2005].

the overall eruptive energy inferred in the previous section, but it is close to the median of the twelve examples for various eruptions given by *Johnson* [2003].

[14] The explosion energy inferred here is a crude estimate, and is subject to various factors not sufficiently addressed in the present study. From field experiments, *Goto et al.* [2001] found that the scaled depth of the explosion controls the energy partition to the airwave. Unknown difference in this parameter between the Asama and the mine blast cases may have resulted in significant under- or overestimate of the energy. Other sources of error may include space-time variability of sound velocity structure, and zonal and meridional wind at ionospheric heights. Clarifications of these factors would make GPS-TEC a more reliable approach to estimate volcanic explosion energies.

[15] **Acknowledgment.** I thank Naoyuki Fujii for encouraging this study and Edvard L. Afraimovich for constructive comments.

## References

Afraimovich, E. L., E. A. Kosogorov, and O. S. Lesyuta (2002), Effects of the August 11, 1999, total solar eclipse as deduced from total electron content measurements at the GPS network, *J. Atmos. Sol. Terr. Phys.*, *64*, 1933–1941.

Artru, J., V. Ducic, H. Kanamori, P. Lognonné, and M. Murakami (2005), Ionospheric detection of gravity waves induced by tsunamis, *Geophys. J. Int.*, *160*, 840–848.

Calais, E., and J. B. Minster (1995), GPS detection of ionospheric perturbations following the January 17, 1994, Northridge earthquake, *Geophys. Res. Lett.*, *22*, 1045–1048.

Calais, E., J. B. Minster, M. A. Hofton, and H. Hedlin (1998), Ionospheric signature of surface mine blasts from Global Positioning System measurements, *Geophys. J. Int.*, *132*, 191–202.

Ducic, V., J. Artru, and P. Lognonné (2003), Ionospheric remote sensing of the Denali earthquake Rayleigh surface waves, *Geophys. Res. Lett.*, *30*(18), 1951, doi:10.1029/2003GL017812.

Fitzgerald, T. J. (1997), Observations of total electron content perturbations on GPS signals caused by a ground level explosion, *J. Atmos. Sol. Terr. Phys.*, *59*, 829–834.

Georges, T. M. (1968), HF Doppler studies of traveling ionospheric disturbances, *J. Atmos. Terr. Phys.*, *30*, 735–746.

Goto, A., H. Taniguchi, M. Yoshida, T. Ohba, and H. Oshima (2001), Effects of explosion energy and depth to the formation of blast wave and crater: Field explosion experiment for the understanding of volcanic explosion, *Geophys. Res. Lett.*, *28*, 4287–4290.

Heki, K., and J. Ping (2005), Directivity and apparent velocity of coseismic ionospheric disturbances observed with a dense GPS array, *Earth Planet. Sci. Lett.*, *236*, 845–855.

Igarashi, K., et al. (1994), Ionospheric and atmospheric disturbances around Japan caused by th eruption of Mount Pinatubo on 15 June 1991, *J. Atmos. Terr. Phys.*, *56*, 1227–1234.

Johnson, J. B. (2003), Generation and propagation of infrasonic airwaves from volcanic eruptions, *J. Volcanol. Geotherm. Res.*, *121*, 1–14.

Minakami, T. (1942), On the distribution of volcanic ejecta (part 1). The distributions of volcanic bombs ejected by the recent explosions of Asama, *Bull. Earthquake Res. Inst. Univ. Tokyo*, *20*, 65–92.

Nakada, S., M. Yoshimoto, E. Koyama, H. Tsuji, and T. Urabe (2005), Comparative study of the 2004 eruption with old eruptions at Asama Volcano and the activity evaluation (in Japanese with English abstract), *Kazan*, *50*, 303–313.

Roberts, D. H., et al. (1982), A large amplitude traveling ionospheric disturbance produced by the May 18, 1980, explosion of Mount St. Helens, *J. Geophys. Res.*, *87*, 6291–6301.

Tahira, M. (1995), Acoustic resonance of the atmosphere at 3.7 mHz, *J. Atmos. Sci.*, *52*, 2670–2674.

Tsugawa, T., A. Saito, and Y. Otsuka (2004), A statistical study of large-scale traveling ionospheric disturbances using the GPS network in Japan, *J. Geophys. Res.*, *109*, A06302, doi:10.1029/2003JA010302.

Zhang, D. H., and Z. Xiao (2005), Study of ionospheric response to the 4B flare on 28 October 2003 using International GPS Service network data, *J. Geophys. Res.*, *110*, A03307, doi:10.1029/2004JA010738.

K. Heki, Dept. of Natural History Science, Hokkaido University, N10 W8, Kita-ku, Sapporo 060-0810, Japan. (heki@mail.sci.hokudai.ac.jp)